Use of Idempotent Functions in the Aggregation of Different Filters for Noise Removal

Luis González-Jaime[1⋆], Mike Nachtegael[1], Etienne Kerre[1], and Humberto Bustince[2]

[1] Applied Mathematics and Computer Science
{luis.gonzalez, mike.nachtegael, etienne.kerre}@ugent.be
Ghent University, Krijgslaan 281 - S9, 9000 Ghent, Belgium
[2] Departamento de Automática y Computación
bustince@unavarra.es
Universidad Pública de Navarra, Campus Arrosadia, 31006 Pamplona, Spain

Abstract. The majority of existing denoising algorithms obtain good results for a specific noise model, and when it is known previously. Nonetheless, there is a lack in denoising algorithms that can deal with any unknown noisy images. Therefore, in this paper, we study the use of aggregation functions for denoising purposes, where the noise model is not necessary known in advance; and how these functions affect the visual and quantitative results of the resultant images.

Keywords: denoising; idempotent function; aggregation function; OWA operator

1 Introduction

One of the most popular restoration techniques has been, and it is nowadays, the image denoising. No matter how good the capturing process is, an image improvement is always needed. The desired goals of any denoising algorithm are to completely remove noise, while effective information (edge, corner, texture and contrast...) is preserved, at the same time that artifacts do not appear.

Along the years, many algorithms have been proposed by researchers, where the most popular noise assumption is the additive Gaussian noise. However a Gaussian noise [1, 2] assumption is too simplistic for most applications, for instance, for medical or astronomical images [3]. The performance of the algorithms decays drastically when the images are contaminated with a noise distribution for which these algorithms are not reliable. It would be desirable to find a blind denoising algorithm being able to deal with any noise distribution, without any previous knowledge about the noise model. Therefore, we focus our work on the study of the aggregation functions for a set of filtered images previously filtered from a noisy image with unknown noise distribution. Specifically, filters for impulse, Poisson, Gaussian and Rician noise are applied. Then, different aggregation functions are used to verify their behaviour for the denoising task.

⋆ Corresponding author

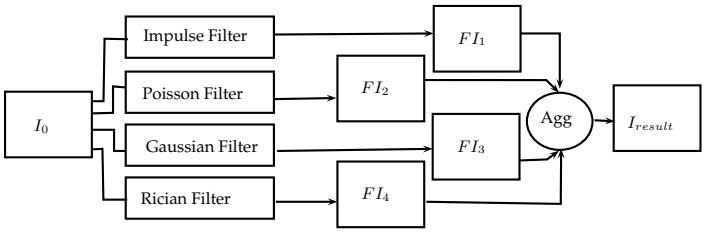

Fig. 1. Schema of the aggregation algorithm

Figure 1 shows the proposed schema. We start from a noisy image I_0, the idea is to use multifuzzy sets to build a new set from the filtered images, so each pixel (i, j) is represented by several values. But, we need to get a single fused image, I_{result}. Thus we use idempotent aggregation functions. In concrete, we select *min*, *max*, *arithmetic mean* and three *OWA operators*. In particular, OWA operators built from fuzzy quantifiers because they provide a more flexible knowledge representation than classic logic [4]. Our aim is to obtain consistent and stable results, regardless of the image nature (e.g. computer tomography (CT), magnetic resonance image (MRI), digital image). Although the main application of this work is with MRI, because they present a more sofisticated noise, it however can be applied to other images with different nature.

The paper is composed as follows: Section 2.1 introduces the different noise models and filters. In Section 2.2, multifuzzy sets are explained. Then, Section 3 presents the idempotent functions and a specific case: the OWAs operators, a family of idempotent averaging functions. Finally, in Sections 4 and 5 specific results and a final conclusion are exposed.

2 Construction of Multifuzzy Sets from a Set of Filtered Images

Given an unknown noisy image, our first step consists in associating a multifuzzy set composed by several images. Each one of these images will be obtained by applying some filter optimized for a certain type of noise.

2.1 Noise Models and Filters

Several approaches exist that deal with Gaussian [1, 2] or impulse noise, although in some cases these are simple approximations compared to the real noise that is presented in the image. For instance, MRI, specifically MR magnitude image, are mainly characterized by Rician noise, although this noise is dependent on the number of coils or the reconstruction method [5]. Furthermore CT, single-photon emission computed tomography (SPECT) or positron emission tomography (PET) are identified by Poisson noise [6, 7]. The selected filters cover different approaches, as well as they perform better for a specific

noise distribution. We give an overview of the characteristics of these filters. The first approach tackles the problem of impulse noise, and uses the DBAIN filter proposed by [8]. The considered filter to deal with white Gaussian noise has been the approach proposed by Goossens et al. [9]. This filter improves the non-local means (NLMeans) filter proposed by Buades et al. [2], dealing with noise in non-repetitive areas with a post-processing step and presenting a new acceleration technique. The approach used to estimate Rician noise is proposed by Aja-Fernandez et al. [10]. This filter adapts the linear minimum mean square error (LMMSE) to Rician distributed images. Finally, for Poisson noise, an extension of the NLMeans is proposed for images damaged by Poisson noise. Deledalle et al. [11] propose to adapt the similarity criteria of NLMeans algorithm to Poisson distribution data. For our experiments, the used parameters are those suggested in the original articles, as the algorithms are tuned to obtain good results.

2.2 Multifuzzy Sets

Once the set of filtered images is obtained, we represent them by means of multifuzzy sets, in which each element is given by a set of n memberships, taking n as the number of filters. A unique multifuzzy set is conformed with all the elements of the images.

Definition 1. *A multifuzzy set of dimension $n \geq 2$ over a finite universe U is defined by a mapping $A : U \to [0,1]^n$ given by $A(u) = (A_1(u), \ldots, A_n(u))$ where each of the A_j for $j = 1, \ldots, n$ is a mapping $A_j : U \to [0,1]$.*

We denote by $\mathcal{M}(U)$ the class of all multifuzzy sets on the referential set U.

Notice that the previous definition is equivalent to the following. Take a family of $n \geq 2$ fuzzy sets $Q_1, \ldots, Q_n$ on the same referential set U. Then a multifuzzy set on U is just the ordered combination of these n fuzzy sets as follows:

$$A = \{(u, A(u)) | u \in U\} \text{ given by } A(u) = (Q_1(u), \ldots, Q_n(u))$$

In this sense, the space of all multifuzzy sets inherits the order from the usual fuzzy sets, which endows it with a partial, bounded order.

In this work, we will deal with two finite referential sets $X = \{0, 1, \ldots, N-1\}$ and $Y = \{0, 1, \ldots, M-1\}$, where N and M are the number of rows and columns of the image, respectively. We will consider multifuzzy sets defined on the Cartesian product $X \times Y$.

Notice that a n dimensional multifuzzy set can also be understood as a type n fuzzy set, as well as an L-fuzzy set with $L = [0,1]^n$ [12].

3 Idempotent functions: building a fuzzy set from multifuzzy sets

When the noisy image is filtered, we get a set of filtered images that composes the multifuzzy set. So, each pixel (i, j) is represented by n values, as many as

filters used. This multifuzzy set needs to be fused in one single image, a fuzzy set. Therefore, we need functions that satisfies one condition: if all the values are the same, the value remains the same. For this reason we decide to use idempotent functions.

Definition 2. *An n-dimensional idempotent function is a mapping* $\gamma : [0,1]^n \to [0,1]$ *such that* $\gamma(x,\dots,x) = x$ *for every* $x \in [0,1]$.

Example 1. An idempotent function is the *mode*, that is the value that occurs most frequently in a data set or a probability distribution.

Remark 1. Notice, that the *mode* from Example 1 is not monotone.

3.1 Construction of idempotent functions

In Proposition 1 we present a new method for constructing idempotent functions.

Proposition 1. *The mapping* $\gamma : [0,1]^n \to [0,1]$ *is an n-dimensional idempotent function if and only if there exist* $f, g : [0,1]^n \to [0,1]$ *such that*

(i) $g(x,\dots,x) \neq 0$ *for every* $x \in [0,1[$*;*
(ii) $f(x,\dots,x) = \frac{x}{1-x} g(x,\dots,x)$ *for* $x \in [0,1[$*,* $f(1,\dots,1) = 1$*,* $g(1,\dots,1) = 0$*;*
(iii) $\gamma(x_1,\dots,x_n) = \frac{f(x_1,\dots,x_n)}{f(x_1,\dots,x_n)+g(x_1,\dots,x_n)}$

Proof. Assume that γ is an n-dimensional idempotent function. Take $f = \gamma$ and $g = 1 - \gamma$. Then

(i) $g(x,\dots,x) = 1 - \gamma(x,\dots,x) = 1 - x \neq 0$ for every $x \in [0,1[$.
(ii) $\frac{x}{1-x} g(x,\dots,x) = \frac{x}{1-x}(1-x) = x = \gamma(x,\dots,x) = f(x,\dots,x)$ and $f(1,\dots,1) = \gamma(1,\dots,1) = 1$ and $g(1,\dots,1) = 0$.
(iii) $\frac{f(x_1,\dots,x_n)}{f(x_1,\dots,x_n)+g(x_1,\dots,x_n)} = \gamma(x_1,\dots,x_n)$.

To see the converse, we only need to check the idempotency. But if γ is defined as in the statement of the proposition, we have that $\gamma(x,\dots,x) = \frac{f(x,\dots,x)}{f(x,\dots,x)+g(x,\dots,x)} = \frac{\frac{x}{1-x} g(x,\dots,x)}{\frac{x}{1-x} g(x,\dots,x)+g(x,\dots,x)}$ which is equal to x for every $x \in [0,1[$. Finally, clearly $\gamma(1,\dots,1) = 1$ □

Example 2.

– Taking $f(x_1,\dots,x_n) = \frac{1}{n}\sum_{i=1}^n x_i$ and $g(x_1,\dots,x_n) = \frac{1}{n}\sum_{i=1}^n (1 - x_i)$ we obtain as idempotent function the *arithmetic mean* (Eq. 1).

$$\gamma_{mean}(x_1,\dots,x_n) = \frac{1}{n}\sum_{i=1}^{n} x_i \tag{1}$$

– Taking $f(x_1, \ldots, x_n) = \sqrt[n]{x_1 \cdot x_2 \cdot \ldots \cdot x_n}$ and
$g(x_1, \ldots, x_n) = \max(1 - x_1, \ldots, 1 - x_n)$ we get Equation 2.

$$\gamma_{root}(x_1, \ldots, x_n) = \frac{\sqrt[n]{x_1 \cdot x_2 \cdot \ldots \cdot x_n}}{\sqrt[n]{x_1 \cdot \ldots \cdot x_n} + \max(1 - x_1, \ldots, 1 - x_n)} \tag{2}$$

Regarding the structure of the space of n-dimensional idempotent functions, we also have the following.

Proposition 2. *Let $\gamma_1, \gamma_2 : [0,1]^n \to [0,1]$ be two n-dimensional idempotent functions. Then:*

1. *$\frac{1}{2}(\gamma_1 + \gamma_2)$ is also an n-dimensional idempotent function;*
2. *$\sqrt{\gamma_1 \gamma_2}$ is also an n-dimensional idempotent function.*

3.2 Idempotent Aggregation Functions: Averaging Functions

Now we study *monotonic non-decreasing idempotent functions*, that are a special case of aggregation functions called *averaging functions*. With these functions we have not only idempotence, but also the result of the function will be bounded by the minimum and maximum of the arguments.

Definition 3. *An aggregation function of dimension n (n-ary aggregation function) is a non-decreasing mapping $f : [0,1]^n \to [0,1]$ such that $f(0, \ldots, 0) = 0$ and $f(1, \ldots, 1) = 1$.*

Definition 4. *An aggregation function $f : [0,1]^n \to [0,1]$ is called averaging or a mean aggregation function if $\min(x_1, \ldots, x_n) \leq f(x_1, \ldots, x_n) \leq \max(x_1, \ldots, x_n)$.*

Proposition 3. *Idempotent monotonic non-decreasing functions and idempotent averaging functions are the same.*

Example 3. Some averaging aggregation functions are the *arithmetic mean* (Eq. 1), *median* (Eq. 3) , *min* or *max*.

$$\gamma_{med}(x_1, \ldots, x_n) = \begin{cases} \frac{1}{2}(x_k + x_{k+1}) & \text{if } n = 2k \\ x_k & \text{if } n = 2k - 1 \end{cases} \tag{3}$$

3.3 Specific Case: OWA Operators and Fuzzy Quantifiers

Introduced by Yager [13], Ordered Weighted Averaging operators, commonly called OWA operators, are a parameterized family of idempotent averaging aggregation functions. They fill the gap between the operators *min* and *max*. The *min*, *max*, *arithmetic mean* or *median* are particular cases of this family.

Definition 5. *[13] A mapping $F : [0,1]^n \to [0,1]$ is called an OWA operator of dimension n if there exists a weighting vector W, $W = (w_1, \ldots, w_n) \in [0,1]^n$ with $\sum_{i=1}^{n} w_i = 1$ and such that $F(a_1, \ldots, a_n) = \sum_{j=1}^{n} w_j b_j$ with b_j the j-th largest of the a_i.*

A natural question is how to obtain the associated weighting vector. Our idea is to calculate the weights for the aggregation operators using linguistic quantifiers, e.g, *about 5*, *a few*, *most*, *nearly half*. The concept of fuzzy quantifiers was introduced by Zadeh [14], offering a more flexible tool for knowledge representation.

Yager suggested an interesting way to compute the weights of the OWA aggregation operator using fuzzy quantifiers [13], which, in the case of an increasing quantifier Q, is given by the expression 4.

$$w_i = Q(\frac{i}{n}) - Q(\frac{i-1}{n}) \qquad Q(r) = \begin{cases} 0 & \text{if } r < a \\ \frac{r-a}{b-a} & \text{if } a \leq r \leq b \\ 1 & \text{if } r > b \end{cases} \tag{4}$$

For the proportional increasing quantifiers, 'at least half' 'as many as possible' and 'most of them', the parameters (a, b) are $(0, 0.5)$, $(0.5, 1)$ and $(0.3, 0.8)$, respectively.

4 Results and Discussion

4.1 How the Algorithm Works: Visual Example

We start from a noisy image contaminated with Rician noise, Figure 2(b). A multifuzzy set is composed with four filtered images (Figures 2(c), 2(d), 2(e), 2(f)) optimized for a certain type of noise. We used the filters proposed in subsection 2.1. Then, we need to build a fuzzy set from the multifuzzy set. For this, we use the idempotent functions. Those defined from the equations 1, 2 and 3, over the multifuzzy set. Each obtained fuzzy set is presented as an image, shown in Figures 3(a), 3(b) and 3(c), respectively.

4.2 Other Experiments

To be able to compare the results to a ground truth, we work with synthetic images artificially corrupted with noise. A magnitude MR volumen originally noise-free (from the BrainWeb database [15]) with 256 gray levels, is corrupted with Rician noise. The noisy images are processed using different filters (see Section 2.1). The aggregation functions used are *min*, *max*, *arithmetic mean* and three OWA operators: *'at least half'*, *'as many as possible'* and *'most of them'* (see Section 3.3).

To quantify the restoration performance of different methods, the PSNR is calculated. This is not bounded. A higher PSNR means better quality. However it is not very well matched to perceived visual quality. This is our motivation to use also other quality indexes. In addition, the Mean Structural Similarity Index (MSSIM) [16] and the Quality Index based on Local Variance (QILV) [17] are used, giving a structural similarity measure. Nonetheless, the former is more sensitive to the level of noise and the latter to any possible blurring of the edges. Both indexes are bounded; the closer to one, the better the image. To avoid any

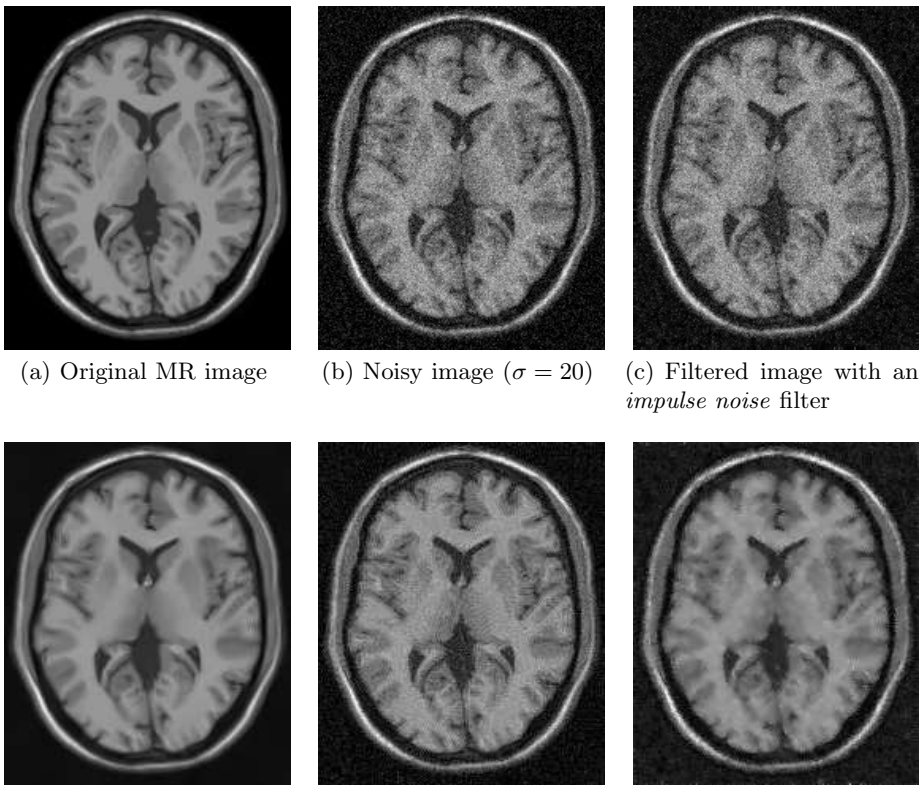

(a) Original MR image (b) Noisy image ($\sigma = 20$) (c) Filtered image with an *impulse noise* filter

(d) Filtered image with a *Gaussian noise* filter (e) Filtered image with a *Poisson noise* filter (f) Filtered image with a *Rician noise* filter

Fig. 2. Synthetic MR brain images (courtesy of Brainweb [15])

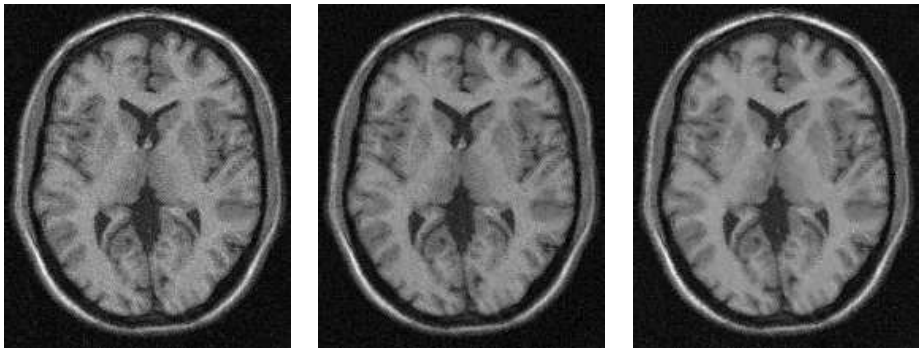

(a) γ_{mean} (b) γ_{root} (c) γ_{median}

Fig. 3. Aggregated images using the Equation 1 (γ_{mean}), Equation 2 (γ_{root}) and Equation 3 (γ_{median}).

bias due to background, the quality measures are only applied to those areas of the image that are relevant.

Two experiments were accomplished with noisy images corrupted with Rician noise, with $\sigma = 10$ and $\sigma = 20$. Table 4.2 shows that the Gaussian filter obtains the best results. However, the visual quality shows in Figure 4(b), that this filter over-filtered and blurries some regions, especially in the borders; consequently it looses some important details (Figure 4(a)). On the other side, Rician filter preserves more details (Figure 4(c)), although visually it is less pleasant and almost does not filter close to the borders. Curiously, the Poisson filter obtains also good results, although the filter is not optimal for this type of noise; it mainly over-filters (Figure 4(d)). It also shown that results get affected when the noise level increases, since aggregation functions fuses the filtered images, that also get affected by noise. The statistics for the aggregation functions are quite similar, although their visual appearances are totally different. The min, max or OWA 'at least half' present images that after being aggregated still look like are contaminated with impulse noise. These results are not interesting for denoising. However some areas, close to the borders, are better defined for these functions (Figures 4(f) and 4(g)), except for the presence of undesired noise. On the other side, the arithmetic mean or the OWA 'as many as possible' show a better compromise between the visual and quantitative quality (Figures 4(e) and 4(i)).

We presented an approach that is noise type independent. For this reason, Table 2 also shows the use of the same algorithm for the same MR volumen contaminated with Poisson noise[3]. The results show that some aggregation functions, as the mean or 'OWA most of them', obtain comparable results to the Poisson filter.

5 Conclusion

The use of multifuzzy sets for denoising purposes is probed, how these sets can be merged in a final fuzzy set (an image) using idempotent aggregation functions. The results show that choosing the right function can provide good results, comparable to the best considered filter, although the result will never be as good as the best filter by the cooperation characteristics of aggregation functions. The different studied functions present different characteristics. For instance, the arithmetic mean operator finds a compromise, while the min or max present better defined borders, despite of a poor global quality. The presented algorithm is used with four different filters, although further research can be done using more and/or new filters; or new aggregation functions. Moreover, a new challenge arises where different functions can be combined on a multifuzzy set. In other words, the best aggregation function is chosen for each pixel, looking for a compromise and presenting a new tool for blind denoising.

[3] It is known that MR images are not contaminated with Poisson noise, but this was carried out for study purposes.

Table 1. Results for the MR volumen, which contains 181 MR images contaminated with Rician noise with $\sigma = 10$ and $\sigma = 20$.

	$\sigma = 10$						$\sigma = 20$					
Filter	PSNR		MSSIM		QILV		PSNR		MSSIM		QILV	
	mean	std	mean	std	mean	std	mean	std	mean	std	mean	std
Noisy	30.803	1.951	0.871	0.043	0.970	0.056	24.866	1.986	0.720	0.089	0.826	0.154
Impulse	30.803	1.960	0.872	0.972	0.043	0.053	24.906	2.005	0.720	0.089	0.835	0.150
Poisson	35.395	2.089	0.960	0.015	0.991	0.008	27.840	1.915	0.808	0.062	0.940	0.114
Gaussian	**36.966**	2.900	**0.970**	0.013	**0.994**	0.004	**32.629**	2.483	**0.927**	0.030	**0.970**	0.021
Rician	33.446	2.370	0.942	0.019	**0.994**	0.004	26.758	2.139	0.779	0.072	0.920	0.103
γ_{min}	33.128	2.273	0.930	0.026	**0.994**	0.006	27.736	2.347	0.823	0.063	0.965	0.048
γ_{max}	32.261	1.970	0.921	0.026	0.990	0.020	26.107	1.892	0.795	0.065	0.940	0.109
γ_{mean}	34.530	2.121	0.939	0.020	**0.994**	0.008	28.621	2.057	0.822	0.059	0.961	0.070
γ_{OWA_half}	32.830	1.992	0.928	0.023	0.991	0.017	26.915	1.911	0.802	0.063	0.944	0.100
γ_{OWA_many}	33.650	2.250	0.934	0.023	**0.994**	0.006	28.257	2.272	0.822	0.061	0.963	0.057
γ_{OWA_most}	34.324	2.114	0.940	0.019	**0.994**	0.008	28.291	2.064	0.815	0.061	0.954	0.079

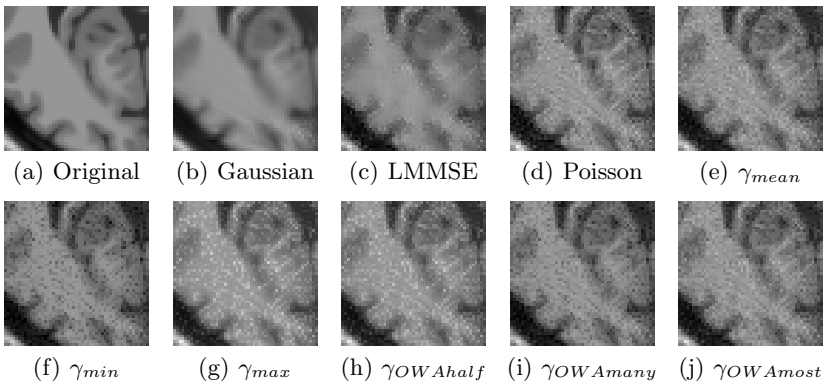

(a) Original (b) Gaussian (c) LMMSE (d) Poisson (e) γ_{mean}

(f) γ_{min} (g) γ_{max} (h) $\gamma_{OWAhalf}$ (i) $\gamma_{OWAmany}$ (j) $\gamma_{OWAmost}$

Fig. 4. Region cropped from a MR brain image. These are the results for the filtered and aggregated images from a noisy image contaminated with $\sigma = 20$.

Table 2. Results for the MR volumen, which contains 181 MR images contaminated with Poisson noise. Legend: (a) Noisy; (b) Impulse; (c) Poisson; (d) Gaussian; (e) Rician; (f) γ_{min}; (g) γ_{max}; (h) γ_{mean}; (i) γ_{OWA_half}; (j) γ_{OWA_many}; (k) γ_{OWA_most}.

Filter	PSNR		MSSIM		QILV		Filter	PSNR		MSSIM		QILV	
	mean	std	mean	std	mean	std		mean	std	mean	std	mean	std
(a)	31.314	2.661	0.883	0.051	0.977	0.023	(g)	32.501	2.887	0.925	0.035	0.993	0.005
(b)	31.290	2.650	0.883	0.052	0.978	0.024	(h)	35.293	2.836	0.941	0.028	**0.995**	0.002
(c)	**36.964**	3.496	**0.970**	0.015	0.993	0.004	(i)	32.993	2.816	0.927	0.034	0.993	0.005
(d)	34.166	3.021	0.941	0.028	0.967	0.022	(j)	33.129	2.737	0.929	0.033	0.991	0.004
(e)	31.314	2.661	0.883	0.052	0.977	0.024	(k)	34.807	2.797	0.937	0.030	**0.995**	0.002
(f)	32.488	2.660	0.928	0.032	0.985	0.010							

Acknowledgement This work is supported by the European Commission under contract no. 238819 (MIBISOC Marie Curie ITN) and by the National Science Foundation of Spain, reference TIN2010-15055.

References

1. L. I. Rudin, S. Osher, E. Fatemi, Nonlinear total variation based noise removal algorithms, Physica D 60 (1-4).
2. A. Buades, B. Coll, J. M. Morel, A review of image denoising algorithms, with a new one, Multiscale Modeling & Simulation 4 (2).
3. R. Molina, J. Nunez, F. J. Cortijo, J. Mateos, Image restoration in astronomy - A Bayesian perspective, IEEE Signal Processing Magazine 18 (2).
4. F. Chiclana, F. Herrera, E. Herrera-Viedma, Integrating three representation models in fuzzy multipurpose decision making based on fuzzy preference relations, Fuzzy Sets and Systems 97 (1).
5. S. Aja-Fernandez, A. Tristan-Vega, C. Alberola-Lopez, Noise estimation in single- and multiple-coil magnetic resonance data based on statistical models, Magnetic Resonance Imaging 27 (10).
6. S. Suzuki, A comparative-study on pre-smoothing techniques for projection data with poisson noise in computed-tomography, Optics Communications 55 (4).
7. M. S. Rosenthal, J. Cullom, W. Hawkins, S. C. Moore, B. M. W. Tsui, M. Yester, Quantitative SPECT imaging - A review and recommendations by the focus committee of the society-of-nuclear-medicine computer and instrumentation council, Journal of Nuclear Medicine 36 (8).
8. K. S. Srinivasan, D. Ebenezer, A new fast and efficient decision-based algorithm for removal of high-density impulse noises, IEEE Signal Processing Letters 14 (3).
9. B. Goossens, Q. Luong, A. Pizurica, W. Philips, An improved non-local denoising algorithm, in: Local and Non-Local Approximation in Image Processing, International Workshop, Proceedings, 2008, pp. 143–156.
10. S. Aja-Fernandez, C. Alberola-Lopez, C.-F. Westin, Noise and signal estimation in magnitude MRI and Rician distributed images: A LMMSE approach, IEEE Transactions on Image Processing 17 (8).
11. C.-A. Deledalle, F. Tupin, L. Denis, Poisson NL means: Unsupervised non local means for poisson noise, in: 2010 IEEE International Conference on Image Processing, IEEE, 2010.
12. G. J. Klir, B. Yuan, Fuzzy sets and fuzzy logic, Prentice Hall New Jersey, 1995.
13. R. R. Yager, On ordered weighted averaging aggregation operators in multicriteria decision-making, IEEE Transactions on Systems Man and Cybernetics 18 (1).
14. L. A. Zadeh, A computational approach to fuzzy quantifiers in natural languages, Computers & Mathematics with applications 9 (1).
15. BrainWeb: Simulated Brain Database.
URL `http://mouldy.bic.mni.mcgill.ca/brainweb/`
16. Z. Wang, A. C. Bovik, H. R. Sheikh, E. P. Simoncelli, Image quality assessment: from error visibility to structural similarity, IEEE Transactions on Image Processing 13 (4) (2004) 600–612.
17. S. Aja-Fernandez, R. S. J. Estepar, C. Alberola-Lopez, C. F. Westin, Image quality assessment based on local variance, in: Conference Proceedings. Annual Intl. Conf. of the IEEE Engineering in Medicine and Biology Society, 2006.